IMEX Runge-Kutta Parareal for Dispersive Problems

Tommaso Buvoli[1] and Michael Minion[2]

[1] University of California, Merced, Merced CA 95343, USA,
tbuvoli@ucmerced.edu,
[2] Lawrence Berkeley National Lab, Berkeley, CA 94720, USA,
mlminion@lbl.gov.

Abstract. Parareal is a widely studied parallel-in-time method that can achieve meaningful speedup on certain problems. However, it is well known that the method typically performs poorly on dispersive equations. This paper analyzes linear stability and convergence for IMEX Runge-Kutta parareal methods on dispersive equations. By combining standard linear stability analysis with a simple convergence analysis, we find that certain parareal configurations can achieve parallel speedup on dispersive equations. These stable configurations all posses low iteration counts, large block sizes, and a large number of processors.

Keywords: parareal, parallel-in-time, implicit-explicit, high-order, dispersive equations

1 Introduction

The numerical solution of ordinary and partial differential equations (ODEs and PDEs) is one of the fundamental tools for simulating engineering and physical systems whose dynamics are governed by differential equations. Examples of fields where PDEs are used span the sciences from astronomy, biology, and chemistry to zoology, and the literature on methods for ODEs is well established (see e.g. [10,11]).

Implicit-explicit or IMEX methods are a specialized class of ODE methods, that are appropriate for problems where the right-hand side of the equation can be additively split into two parts, one of which is treated explicitly and one implicitly. IMEX methods are most often used for equations where the splitting can be done so that the implicit terms are linear and the non-stiff terms are nonlinear, thus avoiding the need to solve a coupled nonlinear implicit equation in the time step. The canonical example is nonlinear advection-diffusion type equations, where the stiffness comes from the (linear) diffusion terms and the nonlinear terms can be treated explicitly. IMEX methods are hence popular in many fluid dynamics settings. Second-order methods based on a Crank-Nicolson treatment of the diffusive terms and an explicit treatment of the nonlinear terms are a notable example. However in this study, we consider a different class of problems where the IMEX schemes are applied to a dispersive rather than diffusive term. Here a canonical example is the non-linear Schrödeinger equation. Within the class of IMEX methods, we restrict the study here to those based on additive or IMEX Runge-Kutta methods. (See e.g.[1,5,12,3].) In particular, we will study the behavior of the the parallel in time method, parareal, constructed from IMEX Runge-Kutta (here after IMEX-RK) methods applied to dispersive problems.

Parallel-in-time methods, date back at least to the work of Nievergelt in 1964 [15], but has seen a resurgence of interest in the last two decades [9]. The parareal method introduced in 2001 [13], is perhaps the most well know parallel-in-time method, and can be arguably attributed to catalyzing the recent renewed interest in temporal parallelization. The emergence of parareal also roughly coincides with the end of the exponential increase in individual processor speeds in massively parallel computers, a development that has resulted in a heightened awareness of the bottleneck to reducing run time for large scale PDE simulations through spatial parallelization techniques alone. Parareal is a relatively simple method to implement (see Section 3), and can in principle be employed using any single-step serial temporal method, although one main theme of this paper is that the choice of method is critical to the performance of the parareal.

Parareal employs a concurrent iteration over multiple time steps to achieve parallel speed up, and one of the main drawbacks of the parareal method is that the parallel efficiency is typically quite modest and is formally bounded by the inverse of the number of iterations required to converge to the specified tolerance to the serial solution. As will be shown, the convergence properties of the parareal methods considered here are quite complex, hence the efficiency of parareal depends sensitively on the problem being considered, the accuracy desired, and the choice of parameters determining the parareal method. In practice, this makes the parallel performance of parareal difficult to summarize succinctly. Another well known problem with parareal is that the convergence of the method performs much better for purely diffusive problems compared to advective or dispersive equations.

An alternative to viewing parareal as an iterative parallel method for converging to some serial solution is to consider parareal with a fixed number of iterations as a one-step method with parallelization across the method. A fixed number of parareal iterations using a Runge-Kutta method can in fact be formulated as a different (rather complicated) Runge-Kutta method. Taking this point of view, one can consider the accuracy and stability in the classical sense using the scalar Dahlquist test problem, and the parallel cost of the method is essentially known *apriori* making comparisons in terms of accuracy versus wall-clock more straightforward.

We present studies that combine convergence and the classical linear stability diagrams of parareal on the Dahlquist problem. The results can be quite surprising, including the possibility that the parareal iterations can converge to a method that is unstable in the classical sense. We can also identify the types of problems and parameter choices for which parareal should provide some speedup for purely dispersive problems. Additionally, the beneficial role of adding diffusion to the problem can be easily demonstrated using our analysis.

The rest of this paper is organized as follows. In the next section, a general overview of IMEX-RK methods is presented, and the specific methods used in our study are identified. In Section 3, a short review of the parareal method is presented followed by a discussion of the theoretical speedup and efficiency of the method. Then in Section 4, a detailed examination of the stability and convergence properties of IMEX-RK parareal methods is presented. Numerical results using the nonlinear Schrödinger equation that confirm some insights from the linear analysis are presented in Section 5. Finally, a review of the relevant findings from this paper and a discussion of open questions is presented in Section 6.

2 IMEX Runge-Kutta Methods

In this section we briefly discuss the IMEX Runge-Kutta (IMEX-RK) methods that are used in this paper. Consider the generic ODE

$$y'(t) = F^E(y,t) + F^I(y,t)$$

where the right hand side can be split in two terms, the first of which, F^E, is assumed to be non-stiff and hence treated explicitly while the second is treated implicitly. The simplest such method is forward/backward Euler

$$y_{n+1} = y_n + \Delta t \left(F^E(y_n, t_n) + F^I(y_{n+1}, t_{n+1}) \right).$$

In each step, one needs to evaluate $F^E(y_n, t_n)$ and then solve the implicit equation

$$y_{n+1} - \Delta t F^I(y_{n+1}, t_{n+1}) = y_n + \Delta t F^E(y_n, t_n)$$

Higher-order IMEX methods can be constructed using different families of integrators and IMEX-RK methods (also called *additive* or *partitioned*) are one popular choice (see e.g. [1,5,12,3]). The generic form for an S stage IMEX RK method is

$$y_{n+1} = y_n + \Delta t \left(\sum_{j=1}^{S} b_j^E F^E(y_j, t_j) + b_j^I F^I(y_j, t_j) \right)$$

where the stage values are

$$y_s = y_n + \Delta t \left(\sum_{j=1}^{s-1} a_{s,j}^E F^E(y_j, t_j) + \sum_{j=1}^{s} a_{s,j}^I F^I(y_j, t_j) \right).$$

Such methods are typically encoded in the Butcher matrices containing $a_{s,j}^E$ and $a_{s,j}^I$. As with the Euler method, each stage of an IMEX method requires the evaluation of $F^E(y_j, t_j)$, $F^I(y_j, t_j)$ and the solution of the implicit equation

$$y_s - (\Delta t a_{s,s}^I) F^I(y_s, t_s) = r_s. \tag{1}$$

IMEX methods are particularly attractive when $F^I(y,t) = Ly$, where L is a linear operator so that (1) becomes

$$(I - \Delta t a^I_{s,s} L) y_s = r_s. \tag{2}$$

If a fast preconditioner is available for inverting these systems, or if the structure of L is simple (e.g. diagonal), then IMEX methods can provide significant computational savings compared to fully implicit methods.

To achieve a certain order of accuracy, the coefficients a^E and a^I must satisfy both order and matching conditions. Unfortunately, the total number of conditions grows extremely fast with the order of the method, rendering classical order-based constructions difficult. To the best of the authors' knowledge there are currently no IMEX methods beyond order five that have been derived using classical order conditions. However, by utilizing different approaches, such as extrapolation methods [6] or spectral deferred correction [7,14], it is possible to construct high-order IMEX methods.

In this work, we consider IMEX-RK methods of order one through four. The first and second order methods are the (1,1,1) and (2,3,2) methods from [1] whose tableaus can be found in Section 2.1 and Section 2.5 respectively. The third and fourth order methods are the ARK3(2)4L[2]SA and ARK4(3)6L[2]SA from [12]. All the schemes we consider have an L-Stable implicit integrator.

3 The parareal method

The parareal method, first introduced in 2001 [13], is a popular approach to time parallelization of ODEs. In this section, we will give a brief over-view of parareal and then present a theoretical model for the parallel efficiency and speedup of the method.

3.1 Method definition

In the original form, parareal is straight-foward to describe by a simple iteration. Let $[T_0, T_f]$ be the time interval of interest, and t_n denote a series of time steps in the interval. Next, define coarse and fine propagators $\mathcal{G}$ and $\mathcal{F}$, each of which produces an approximation to the ODE at t_{n+1} given an approximation to the solution at t_n. The goal of parareal is to iteratively compute an approximation to the numerical solution that would result from applying $\mathcal{F}$ sequentially on each time interval

$$y_{n+1} = \mathcal{F}(y_n) \tag{3}$$

Assume that one has a provisional guess of the solution at each t_n, denoted y_n^0. This is usually provided by a serial application of the coarse propagator $\mathcal{G}$. Then the kth parareal iteration is given by

$$y^{k+1}_{n+1} = \mathcal{F}(y^k_n) + \mathcal{G}(y^{k+1}_n) - \mathcal{G}(y^k_n), \tag{4}$$

where the critical observation is that the $\mathcal{F}(y_n^k)$ terms can be computed on each time interval in parallel. As shown below, assuming that $\mathcal{G}$ is computationally much less expensive than $\mathcal{F}$ and the method converges in few enough iterations, parallel speedup can be obtained.

Part of the appeal of the parareal method is that the propagators $\mathcal{G}$ and $\mathcal{F}$ are not constrained by the definition of the method. Hence, parareal as written can in theory be easily implemented using any numerical ODE method for $\mathcal{G}$ and $\mathcal{F}$. Unfortunately, as discussed below, not all choices lead to efficient or even convergent parallel numerical methods, and the efficiency of the method is sensitive to the choice of parameters.

Note that as described, the entire parareal method can be considered as a self-starting, single step method for the interval $[T_0, T_f]$ with time step $\Delta T = T_f - T_0$. In the following Section, the classical linear stability of parareal as a single step method will be considered for $\mathcal{G}$ and $\mathcal{F}$ based on IMEX-RK integrators. This perspective also highlights the fact that there is a choice that must be made for any particular parareal run regarding the choice of ΔT. To give a concrete example for clarity, suppose the user has an application requiring 1024 time steps of some numerical method to compute the desired solution on the time interval $[0, 1]$, and that 8 parallel processors are available. She could then run the parareal algorithm on 8 processors with 128 steps of the serial method corresponding to $\mathcal{F}$. Alternatively, parareal could be run as a single step method on two *blocks* of time steps corresponding to $[0, 1/2]$ and $[1/2, 1]$ with each block consisting to 512 serial fine time steps, or 64 serial steps corresponding to $\mathcal{F}$ for each processor on each block. These two blocks would necessarily be computed serially with the solution from the first block at $t = 1/2$ serving as the initial initial condition on the second block. It might seems counter- intuitive that the second approach would lead to a more efficient method, but in the following we will show that this can be the case. The cause of this is the fact that the number of iterations needed for parareal to converge typically increases with the length of the time interval over which it is applied.

3.2 Cost and theoretical and parallel speedup

We describe a general framework for estimating the potential speedup for the parareal method. For simplicity, assume that an initial value ODE is to be solved with some method requiring N_S time steps to complete the simulation on the interval $[0, T_f]$. We assume further that the the same method will be used in the fine propagator in parareal. If each step of the serial method has cost $c_{\mathcal{F}}$, then the total serial cost is

$$C_S = N_S c_{\mathcal{F}}. \tag{5}$$

In the present context, both the coarse and fine propagators consist of a number of steps of an IMEX-RK method applied to a pseudo-spectral discretization of a PDE. The main cost in general is then the cost of the FFT used to compute explicit nonlinear spatial function evaluations. Hence each step of either an IMEX-RK method has essentially a fixed cost. This is in contrast to the case where implicit equations are solved with an iterative method and the cost per time step $c_{\mathcal{F}}$ could vary considerably by step.

Given N_p available processors, the parareal algorithm can be applied to N_b blocks of time intervals, with each block having length $\Delta T = T_f/N_b$. Again for simplicity we assume that in each time block, each processor is assigned a time interval of equal size $\Delta T_P = \Delta T/N_p$. Under these assumptions, $\mathcal{F}$ is now determined to be $N_{\mathcal{F}} = N_S/(N_p N_b)$ steps of the serial method. Parareal is then defined by the choice of $\mathcal{G}$, which we assume here is constant across processors and blocks consisting of $N_{\mathcal{G}}$ steps of either the same, or different RK method as used in $\mathcal{F}$ with cost per step $c_{\mathcal{G}}$. Let C_F be the time needed to compute $\mathcal{F}$

$$C_F = N_{\mathcal{F}} c_{\mathcal{F}} = \frac{N_S}{N_p N_b} c_{\mathcal{F}}. \tag{6}$$

Likewise, let $C_G = N_{\mathcal{G}} c_{\mathcal{G}}$ be the cost of the coarse propagator per block.

The cost of K iterations of parareal performed on a block is the sum of the cost of the predictor on a block, $N_p C_G$, plus the additional cost of each iteration. In an ideal setting where each processor computes a quantity as soon as possible and communication cost is neglected, the latter is simply the $K(C_F + C_G)$. Hence the total cost of parareal on a block is

$$C_B = N_p C_G + K(C_F + C_G) \tag{7}$$

The total cost of parareal is the sum over blocks

$$C_p = \sum_{i=1}^{N_b} \left(N_p C_G + K_i(C_F + C_G)\right) = N_b N_p C_G + (C_F + C_G) \sum_{i=1}^{N_b} K_i \tag{8}$$

where K_i is the number of iterations required to converge on block i. Let $\bar{K}$ denote the average number of iterations across the blocks

$$\bar{K} = \frac{1}{N_b} \sum_{i=1}^{N_b} K_i, \tag{9}$$

then

$$C_p = N_b \left(N_p C_G + \bar{K}(C_F + C_G)\right) \tag{10}$$

Note the first term $N_b N_p C_G$ is exactly the cost of applying the coarse propagator over the entire time interval.

To define the speedup $S = C_s/C_p$, first note

$$C_S = N_S c_{\mathcal{F}} = N_b N_p N_{\mathcal{F}} c_{\mathcal{F}} = N_b N_p C_F, \tag{11}$$

so that

$$S = \frac{N_b N_p C_F}{N_b \left(N_p C_G + \bar{K}(C_F + C_G)\right)} \tag{12}$$

To simplify, denote $\alpha = C_G/C_F$, giving

$$S = \frac{N_p}{N_p\alpha + \bar{K}(1+\alpha)} \tag{13}$$

The parallel efficiency of parareal $E = S/N_p$ is

$$E = \frac{1}{(N_p + \bar{K})\alpha + \bar{K}}. \tag{14}$$

A few immediate observation can be made from the formulas for S and E. Clearly the bound on efficiency is $E < 1/\bar{K}$. Further, if significant speedup is to be achieved, it should be true that $\bar{K}$ is significantly less than N_p and $N_p\alpha$ is small as well. As will be demonstrated later, the total number of parareal iterations required is certainly problem dependent and also dependent on the choices of $\mathcal{F}$ and $\mathcal{G}$. It might seem strange at first glance that the number of blocks chosen does not appear explicitly in the above formulas for S and E. Hence it would seem better to choose more blocks of shorter length so that $\bar{K}$ is minimized. Note however that increasing the number of blocks by a certain factor with the number of processors fixed means that $N_{\mathcal{F}}$ will decrease by the same factor. If the cost of the coarse propagator C_G is independent of the number of blocks (as in the common choice of $\mathcal{G}$ being a single step of a given method, i.e., $N_{\mathcal{G}} = 1$), then α will hence increase by the same factor. Lastly, one can derive the total speedup by also considering the speedup over each block, S_i as

$$S = \frac{1}{\sum_{i=1}^{N_b} \frac{1}{N_b S_i}} = \frac{1}{\frac{1}{N_b}\sum_{i=1}^{N_b} \frac{1}{S_i}}$$

Note: Mention 1 block or constant K

4 Dispersive Dalquist: stability, convergence, accuracy

An effective parareal integrator must converge rapidly and maintain stability. Previous studies have looked at convergence and stability of parareal on the bounded and unbounded intervals as the iterations k tends to infinity [8] and for parareal with fixed parameters [2,17]. However, these works primarily focus on diffusive problems. A more recent work that addressed dispersive equations is [16] from which we will base our own analysis.

In this section, we analyze these properties for IMEX-RK parareal methods using the dispersive partitioned Dahlquist test problem

$$\begin{cases} y' = i\lambda_1 y + i\lambda_2 y \\ y(t_0) = y_0 \end{cases} \qquad \lambda_1, \lambda_2 \in \mathbb{R}, \tag{15}$$

where the term $i\lambda_1 y$ is treated implicitly and the term $i\lambda_2 y$ is treated explicitly.

When solving (15), all one-step integrators reduce to an iteration of the form

$$y_{n+1} = R(iz_1, iz_2)y_n \quad \text{where} \quad z_1 = h\lambda_1,\ z_2 = h\lambda_2, \tag{16}$$

and $R(\zeta_1, \zeta_2)$ is the stability function of the method. Since RK-based parareal is also a one-step method it reduces to the iteration (16); however, the index n now indicates the number of parareal blocks. The stability function $R(\zeta_1, \zeta_2)$ plays an important role for both convergence and stability of parareal. The approach we take for determining the stability functions and convergence rate is identical to the one presented in [16].

4.1 Convergence

A parareal method will always converge to the fine solution after N_p iterations. However, to obtain parallel speedup, one must achieve convergence in substantially fewer iterations. Convergence rates for a linear problem can be studied by expressing the parareal iteration in matrix form, and computing the maximal singular values of the parareal iteration matrix [16]. Below, we summarize the key formulas behind this observation.

For the linear problem (15) the parareal iteration (4) reduces to

$$\mathbf{M}_g \mathbf{y}^{k+1} = (\mathbf{M}_g - \mathbf{M}_f)\mathbf{y}^k + \mathbf{b}$$

where $\mathbf{y} = [y_0, y_1, y_2, \ldots, y_{N_p}]^T$ is a vector containing the approximate parareal solutions at each fine timestep, the matrices $\mathbf{M}_g, \mathbf{M}_f \in \mathbb{R}^{p+1,p+1}$ and the vector $\mathbf{b} \in \mathbb{R}^{p+1}$ are

$$\mathbf{M}_f = \begin{bmatrix} I & & & \\ -F & I & & \\ & \ddots & \ddots & \\ & & -F & I \end{bmatrix} \qquad \mathbf{M}_g = \begin{bmatrix} I & & & \\ -G & I & & \\ & \ddots & \ddots & \\ & & -G & I \end{bmatrix} \qquad \mathbf{b} = \begin{bmatrix} y_0 \\ 0 \\ \vdots \\ 0 \end{bmatrix} \tag{17}$$

and the constants $F = R_F(iz_1, iz_2)^{N_F}$ and $G = R_G(iz_1, iz_2)^{N_C}$ are the stability functions for the fine and coarse integrators. The parareal algorithm can now be interpreted as a fixed point iteration that converges to the fine solution

$$\mathbf{y}_F = \left[1, F, F^2, \ldots, F^{N_p}\right]^T y_0$$

and whose error $\mathbf{e}_k = \mathbf{y}^k - \mathbf{y}_F$ evolves according to

$$\mathbf{e}^k = \mathbf{E}\mathbf{e}^{k-1} \quad \text{where} \quad \mathbf{E} = \mathbf{I} - \mathbf{M}_g^{-1}\mathbf{M}_f. \tag{18}$$

Since parareal converges after N_p iterations, the matrix $\mathbf{E}$ is nilpotent and convergence rates cannot be understood using the spectrum. However, monotonic convergence is guaranteed if $\|\mathbf{E}\| < 1$ since

$$\|e^{k+1}\| \leq \|\mathbf{E}\|\|e^k\| < \|e^k\|,$$

where $\|\cdot\|$ represents any valid norm. We therefore introduce the *convergence region*

$$C_p = \{(z_1, z_2) : \|E\|_p < 1\} \tag{19}$$

that contains the set of all z_1, z_2 where the p-norm of $\mathbf{E}$ is smaller than one and the error iteration (18) is contractive. Note that for rapid convergence that leads to parallel speedup one also needs $\|\mathbf{E}\|_p \ll 1$.

Two-norm for bounding E In [16], Ruprecht selects $\|\mathbf{E}\|_2 = \max_j \sigma_j$, where σ_j is the jth singular value of $\mathbf{E}$. However, the two-norm needs to be computed numerically, which prevents us from understanding the conditions that guarantee fast convergence.

Infinity-norm for bounding E If we consider the ∞-norm, we can exploit the simple structure of the matrix $\mathbf{E}$ to obtain the exact formula

$$\|\mathbf{E}\|_\infty = \frac{1 - |G|^{N_p}}{1 - |G|} |G - F|. \tag{20}$$

See Appendix A for details. By using this exact formula, we can understand the requirements that must be placed on the coarse and fine integrators to guarantee a rapidly convergent parareal iteration. We summarize them in three remarks.

Remark 1. If G is inside its stability region and $|G - F| < \frac{1}{N_p}$ then the parareal iteration converges monotonically. Notice that when $|G| < 1$, then

$$\frac{1 - |G|^{N_p}}{1 - |G|} = \sum_{j=0}^{N_p - 1} |G|^j < N_p.$$

Therefore, $\|\mathbf{E}\| \leq 1$ if $|G - F| < \frac{1}{N_p}$. If we add more processors, then the coarse integrator should more closely approximate the fine solution. One way to accomplish this is by keeping N_T fixed while increasing the number of processors; this shrinks the stepsize of the coarse integrator so that it more closely approximates the fine integrator.

Remark 2. It is more difficult to achieve large convergence regions for a dispersive equation than for a diffusive equation. If we are solving a heavily diffusive problem $y' = \rho_1 y + \rho_2 y$ where $\mathrm{Re}(\rho_1 + \rho_2) \ll 0$ with an accurate and stable integrator, then $G \ll 1$. Conversely, if we are solving a stiff dispersive problem (15) with an accurate and stable integrator we expect that $G \sim 1$. Therefore

$$\frac{1 - |G|^{N_p}}{1 - |G|} \sim \begin{cases} 1 & \text{Diffusive Problem,} \\ N_p & \text{Dispersive Problem.} \end{cases}$$

From this we see that the dispersive case is inherently more difficult since we require that the difference between the coarse integrator and the fine integrator should be much smaller than $\frac{1}{N_p}$ for fast convergence. Moreover, any attempts to pair an inaccurate but highly stable coarse solver ($G \ll 1$) with an accurate fine solver ($F \sim 1$) will at best lead to slow convergence for a dispersive problem since $|G - F| \sim 1$. Rapid convergence is possible if both $|F| \ll 1$ and $|G| \ll 1$, however this is not meaningful convergence since both the coarse and fine integrator are solving the dispersive problem inaccurately.

Remark 3. If G is not stable (i.e. $|G| > 1$), then fast convergence is only possible if F is also unstable so that $|F| > 1$. Convergence requires that the difference between the coarse and fine iterator is sufficiently small so that

$$|G - F| < \frac{1 - |G|}{1 - |G|^{N_p}}.$$

Since G and F are complex numbers we can interpret $\frac{1-|G|}{1-|G|^{N_p}}$ as the radial distance between the numbers. If we want $|F| \leq 1$, then G can never be more than the distance $\frac{1-|G|}{1-|G|^{N_p}}$ from the unit circle. Therefore we require that

$$|G| - \frac{1 - |G|}{1 - |G|^{N_p}} \leq 1 \quad \implies \quad |G| \leq 1.$$

4.2 Linear stability

Linear stability analysis is an important tool for identifying the types of equations that will cause instabilities for a time integrator. The stability region for a one-step IMEX method with stability function $R(\zeta_1, \zeta_2)$ is the region of the complex ζ_1 and ζ_2 plane given by

$$S = \left\{ (\zeta_1, \zeta_2) \in \mathbb{C}^2 : |R(\zeta_1, \zeta_2)| \leq 1 \right\}.$$

Inside S the amplification factor $|R(\zeta_1, \zeta_2)|$ is smaller than or equal to one which ensures that the timestep iteration remains forever bounded. For traditional integrators one normally expects to take a large number of timesteps, so even a mild instability will eventually lead to unusable outputs.

The importance of linear stability for parareal depends on the way the method is run and on the severity of any instabilities. In particular, there are two common approaches for using parareal. In the first approach, one fixes the number of processors and integrates in time using multiple parareal blocks. This turns parareal into a one-step RK method; therefore, if one expects to integrate over many blocks, then the stability region becomes as important as it is for a traditional integrator. An alternative approach is to integrate in time using a single large parareal block. If more accuracy is required, then one simply increases the number of timesteps and processors, and there is never a repeated timestep iteration. In this second scenario we can relax traditional stability requirements since a mild instability in the resulting one-step parareal method will still produce usable results. However, we still cannot ignore large instabilities that amplify the solution by multiple orders of magnitude.

Since we are only looking at the dispersive Dahlquist equation, we restrict ourselves to the following two dimensional stability region

$$S = \left\{ (z_1, z_2) \in \mathbb{R}^2 : |R(iz_1, iz_2)| \leq 1 \right\}. \tag{21}$$

Moreover, all the integrators we considered have stability functions that satisfy

$$R(iz_1, iz_2) = R(-iz_1, -iz_2) \tag{22}$$

which means that we can obtain all the relevant information about stability by only considering S for $z_1 \geq 0$.

A compact formulation of the stability function for a parareal method was derived in [16] and is given by

$$R(iz_1, iz_2) = \mathbf{c}_2 \left(\sum_{j=0}^{k} \mathbf{E}^j \right) \mathbf{M}_g^{-1} \mathbf{c}_1$$

where $\mathbf{M}_g$ is defined in (17), $\mathbf{E}$ is the matrix from (18) and $\mathbf{c}_1 \in \mathbb{R}^{N_p+1}$, $\mathbf{c}_2 \in \mathbb{R}^{1,N_p+1}$ are given by $\mathbf{c_1} = [1, 0, \ldots, 0]^T$ and $\mathbf{c_2} = [0, \ldots, 0, 1]$.

4.3 Linear stability for IMEX-RK

Before presenting results for parareal, we briefly discuss the linear stability properties of the four IMEX-RK methods considered in this work. In Figure 1 we present two-dimensional stability regions (21) and surface plots that show the corresponding amplitude factor. When $z_2 = 0$, IMEX-RK integrators limit to the fully implicit integrator. Since the methods we consider are all constructed using an L-stable implicit method, the amplification factor will limit to zero as $z_1 \to \infty$. This implies that we should not expect good accuracy for large $|z_1|$ since the exact solution always has magnitude one. As expected, this damping occurs at a slower rate for the more accurate high-order methods.

4.4 Linear stability and convergence for parareal

The stability function and convergence rate for a parareal method are dependent on its parameters and on the choice of coarse and fine integrator. Since we are considering RK methods with orders one to four, there are ten possible IMEX-RK pairings where the fine integrator has higher or equivalent order compared to the coarse integrator. The remaining parameters are the number of processors, the number of parareal iterations k, and the number of coarse and fine integrator steps.

In practice, parareal is commonly run with an adaptively selected k that causes the method to keep iterating until a pre-specified residual tolerance is satisfied. When discussing linear stability we instead assume that parareal always performs a fixed number of iterations. This simplifies our analysis and allows us to quantify how iteration count affects stability. Since the matrix $\mathbf{E}$ from (18) does not depend on k, the number of iterations has no effect on the convergence regions. Therefore, our convergence results apply to both non-adaptive and adaptive parareal.

Our aim is to broadly categorize the effect that each of the parameters have on stability and convergence. To reduce the number of total parameters, we

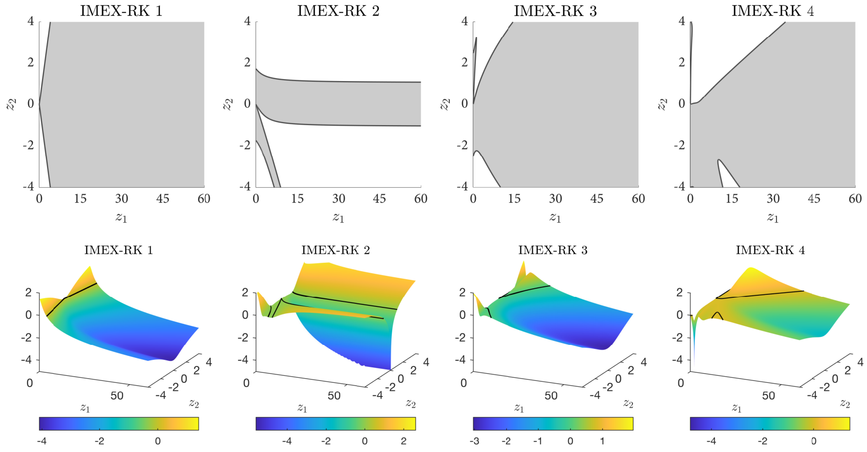

Fig. 1. Dispersive linear stability regions (21) for IMEX-RK methods (top) and surface plots showing $\log(\text{amp}(iz_1, iz_2))$ (bottom). For improved readability we scale the z_1 and z_2 axes differently. For the amplitude function plots, zero marks the cutoff for stability since we are plotting the log of the amplitude function.

always take the number of coarse integrator steps N_C to be one. Even with this simplification there are still too many degrees of freedom to discuss all the resulting parareal methods. Therefore, we only show several example plots that capture the essential phenomena, and provide a set of general remarks to encapsulate our main observations. Those who wish to see additional stability and convergence plots, can download our Matlab code [4] which can be used to generate figures for any other set of parareal parameters.

To showcase the stability and convergence properties of parareal, we present two dimensional plots that overlay the linear stability region (21) and the convergence region (19) with $p = \infty$. We start with a simple example that demonstrates how we construct our plots. Consider the parareal integrator with IMEX-RK3 and IMEX-RK4 as the coarse and fine integrator, respectively, and with parameters $k = 2$, $N_C = 1$, $N_F = 8$, $N_p = 64$. The following three figures show the convergence region (left), the stability region (middle) and an overlay of both (right). Each plot shows the (z_1, z_2) plane where we only consider $z_1 \geq 0$ due to the symmetry condition (22).

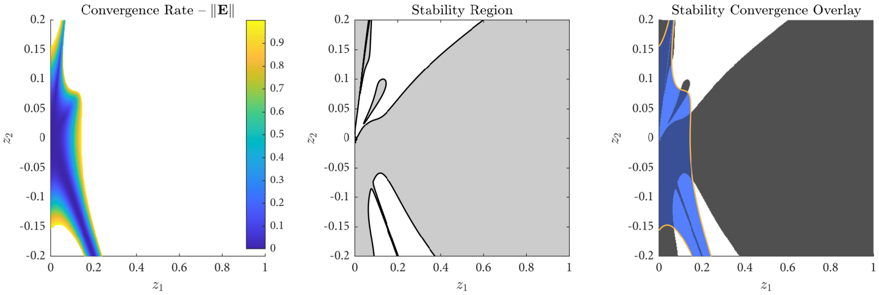

Color	Set	Description
🟦 Light Blue	$C \setminus S$	Contractive iteration, unstable one-step method.
🟦 Dark Blue	$S \cap P$	Contractive iteration, stable one-step method.
⬛ Dark Gray	$S \setminus C$	Non-contractive iteration, stable one-step method.
🟨 Yellow	$\|\mathbf{E}\| = 1$	Boundary of convergence region.

The convergence rate plot has a colorbar that corresponds to the norm of the parareal iteration matrix $\mathbf{E}$ from (18). In the overlay plot there are three distinct regions that are colored according to the legend shown above.

To simply the comparison between different parareal methods, we scale all stability functions relative to the number of fine timesteps N_T; in other words, our plots are generated using the scaled stability function $\widehat{R}(iz_1, iz_2) = R(iN_T z_1, iN_T z_2)$.

For brevity we only present plots for parareal methods with IMEX-RK3 and IMEX-RK4 as the coarse and fine integrator, and with the following parameters:

$$N_T \in \{512, 2048\}, \quad N_p \in \{64, 128, 256, 512\}, \quad k \in \{1, 2, 3, 4\}.$$

In Figures 2 and 3 we show a grid of convergence plots and stability-convergence overlay plots for IMEX parareal integrators with $N_T = 512$ and $N_T = 2048$. Due to the limited stability of the parareal methods near the origin, we magnify the axes in comparison to our plots for IMEX-RK methods. Additional figures for parareal methods with different coarse and fine integrators and with different axes are available in [4].

General remarks on stability and convergence We make several general remarks based on the stability plots shown in Figures 2, 3, and the additional ones contained in [4].

1. There are many regions in the (z_1, z_2) plane where stability and convergence regions do not overlap (in Figures 2, 3 these regions appear in a light blue color). Therefore a parareal method that does not take $k = N_p$ can be unstable even for (z_1, z_2) pairs that are inside the convergence region. If this parareal method is iterated over many blocks, or if the instability is large, then the final output will be unusable. Conversely, lack of convergence paired with stability means that the solution will remain bounded. However

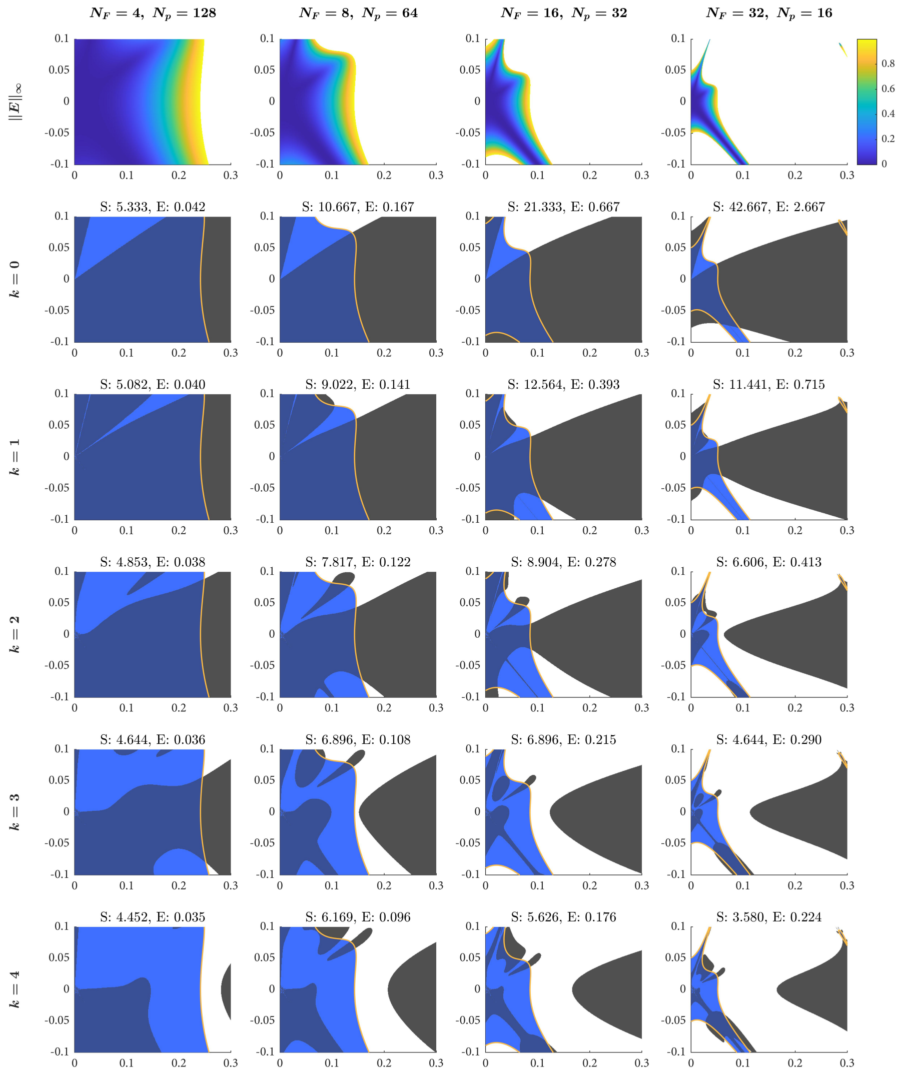

$N_F = 4,\ N_p = 128$ | $N_F = 8,\ N_p = 64$ | $N_F = 16,\ N_p = 32$ | $N_F = 32,\ N_p = 16$

$k = 0$: S: 5.333, E: 0.042 | S: 10.667, E: 0.167 | S: 21.333, E: 0.667 | S: 42.667, E: 2.667

$k = 1$: S: 5.082, E: 0.040 | S: 9.022, E: 0.141 | S: 12.564, E: 0.393 | S: 11.441, E: 0.715

$k = 2$: S: 4.853, E: 0.038 | S: 7.817, E: 0.122 | S: 8.904, E: 0.278 | S: 6.606, E: 0.413

$k = 3$: S: 4.644, E: 0.036 | S: 6.896, E: 0.108 | S: 6.896, E: 0.215 | S: 4.644, E: 0.290

$k = 4$: S: 4.452, E: 0.035 | S: 6.169, E: 0.096 | S: 5.626, E: 0.176 | S: 3.580, E: 0.224

Fig. 2. Stability and convergence overlay plots for parareal configurations with a block size of $N_T = 512$ and IMEX-RK3, IMEX-RK4 as the coarse and fine integrator. The number of processors increases as one moves rightwards in the horizontal direction. The top row shows the convergence rate plot for the method, and all subsequent rows show stability convergence overlays for an increasing number of iterations. The subfigure titles show the speedup (S) and efficiency (E) for each parareal configuration.

the accuracy for these (z_1, z_2) pairs will never surpass that of the coarse integrator unless the number of iterations is large; in many cases as large as $k = N_p$.

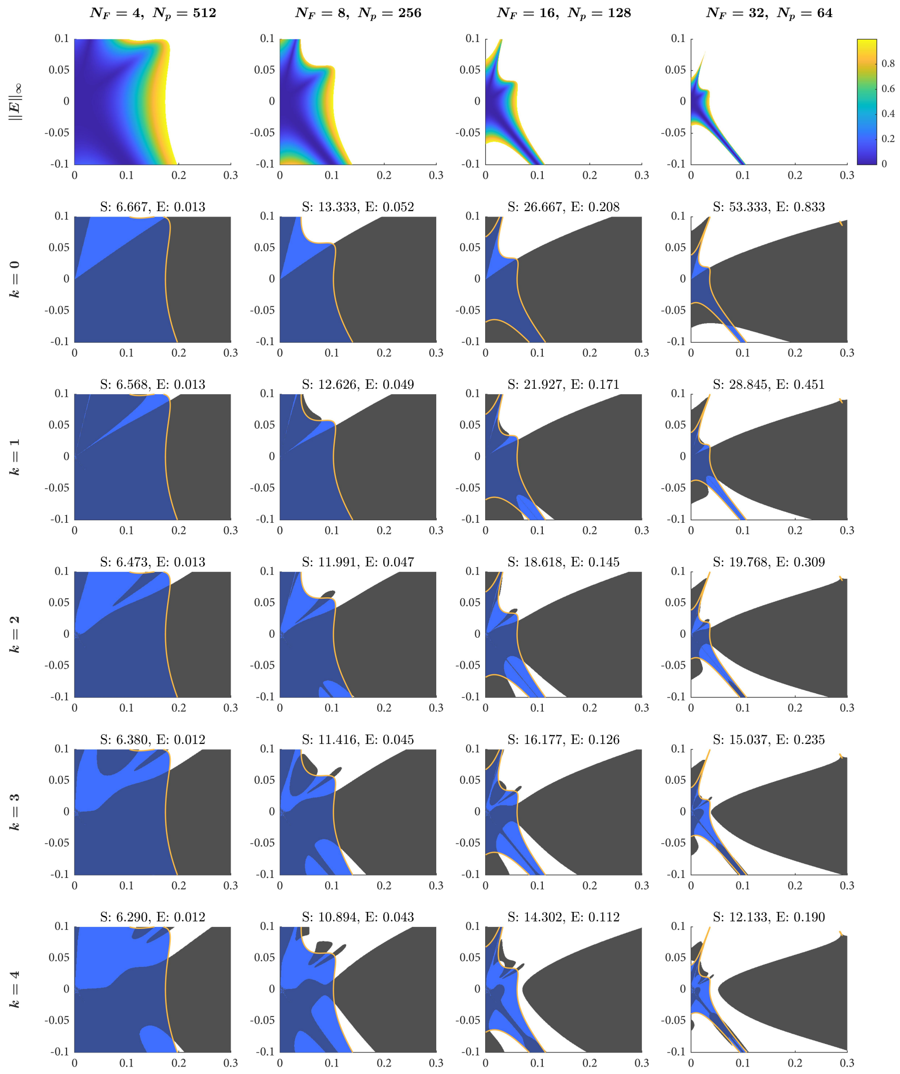

Fig. 3. Stability and convergence overlay plots for parareal configurations with a block size of $N_T = 2048$ and IMEX-RK3, IMEX-RK4 as the coarse and fine integrator.

2. Convergence regions for parareal change drastically depending on the parameters. Overall we see that the choice of coarse integrator and the number of processors have the most prominent effect on the convergence regions near the origin. In particular, the shape of the convergence region appears to be primarily dictated by the choice of coarse integrator, and the size of the region is roughly proportional to the ratio of the number of processors N_p and

the block size N_T. Though one may hope to attain the fastest speedup using a coarse solve with large timesteps, this observation suggests that it is important to carefully balance speedup with the size of the solution spectrum.

3. The choice of fine integrator has almost no effect on the shape or size of the convergence region near the origin. We can understand this by first noticing the convergence region (20) depends on F through the term $|G - F|$. Now, suppose that we select a coarse integrator of order γ, and a fine integrator of order $\gamma + \delta$, where $\delta \geq 0$. If we define $\lambda = z_1 + z_2$, it follows that

$$G = \exp(i\lambda) + \mathcal{O}\left(|\lambda|^{\gamma}\right), \qquad F(\delta) = \exp(i\lambda) + \mathcal{O}\left(|\lambda|^{\gamma+\delta}\right).$$

   Therefore $|G - F(\delta)| = |G - F(0)| + \mathcal{O}\left(|\lambda|^{\gamma}\right)$. This implies that for any choice of fine integrator, the convergence rates will be nearly identical near the (z_1, z_2) origin where λ is small.
4. Stability regions are non-trivial and depend on more parameters than convergence regions. The most significant effect on stability regions is due to the choice of coarse integrator, the number of processors, and the number of parareal iterations.

Remarks regarding IMEX parareal Overall, IMEX parareal methods are not well-suited for dispersive equations. Our main observation is that the stability region splits in two along the z_2 axis; see the bottom right diagrams in Figures 2 and 3 as an example. After searching across many parameters we consistently find that the size of the instability region increases with small N_T, large k, and small N_p (or equivalently large N_F). Nevertheless, IMEX parareal methods can still be effective for solving dispersive equations under three conditions:

1. **Select a stable method pairing.** This is non trivial and many pairings lead to an IMEX parareal method with no stability along the z_2 axis for small k. Of the ten possible coarse-fine integrator pairings, only the ones with IMEX-RK1 or IMEX-RK3 as the coarse integrator were stable. Selecting IMEX-RK2 or IMEX-RK4 as the coarse integrator produced an unstable parareal method for all the parameters we considered. More generally, this suggests that RK pairs should be specially constructed to maximize stability.
2. **Keep the iteration counts low, choose large block lengths, and avoid using too few processors.** Increasing the number of parareal iterations causes the stability region along the z_2 axis to separate. After looking across a wide range of parameters, we find that the stability regions of the IMEX integrators seem to consistently get worse as the number of iterations increase especially if we consider small block lengths N_T or small N_p. This suggests that adaptive implementations of IMEX parareal on dispersive problems will likely lead to an unstable method if the residual tolerance is set too low. However, if one fixes the maximum number of iteration k, selects a large block length N_T, and uses a sufficient number of processors N_p, then the methods can be effective.

3. **Avoid problems with broad spectrums**. Stable pairings of IMEX integrators possess good stability and convergence near the (z_1, z_2) origin. However for all the RK pairings we tested, the convergence regions do not extend far along the z_2 axis. For moderately sized z_2 we consistently see a region of good stability that is paired with non-contractive convergence. These observations suggest that IMEX parareal methods will converge slowly on solutions where the energy is concentrated in these modes. We note that the convergence region is restored as z_2 gets sufficiently large, however in these regions the coarse and fine IMEX integrators both exhibit heavy damping, therefore, rapid convergence to the fine integrator is not a sign of good accuracy; see remark 2 in Section 4.1.

4.5 Accuracy regions for the dispersive Dahlquist equation

To supplement our stability plots we also consider the accuracy regions for IMEX integrators. The accuracy region A_ϵ shows the regions in the $(z_1,\, z_2)$ plane where the difference between the exact solution and the numerical method is smaller than ϵ. The accuracy region for an IMEX method is typically defined as

$$A_\epsilon = \{(z_1, z_2) \in \mathbb{R} : |R(iz_1, iz_2) - \exp(iz_1, iz_2)| \leq \epsilon\},$$

where $R(\zeta_2, \zeta_2)$ is the stability function of the method. Since parareal methods advance the solution multiple timesteps, we scale the accuracy regions by the total number of timesteps in a block so that

$$A_\epsilon = \{(z_1, z_2) \in \mathbb{R} : |R(iN_T z_1, iN_T z_2) - \exp(iN_T z_1, iN_T z_2)| \leq \epsilon\}. \tag{23}$$

Under this scaling, the accuracy region of a fully converged parareal method with $k = N_p$ is

$$A_\epsilon = \left\{(z_1, z_2) \in \mathbb{R} : |R_F(iz_1, iz_2)^{N_T} - \exp(iN_T z_1, iN_T z_2)| \leq \epsilon\right\}.$$

where $R_F(\zeta_1, \zeta_2)$ is the stability function of the fine integrator; this is the accuracy region of a method that consists of N_T steps of the fine integrator.

In Figure 4 we show the accuracy regions for IMEX parareal methods with $N_T = 2048$. The diagrams highlight the importance of the different regions in our stability plots. First, we can clearly see fast convergence to the fine solution inside contractive regions where $\|\mathbf{E}\| \ll 1$. Second, for any $(z_1,\, z_2)$ pairs that are inside the stability region but outside the convergence region, we see that increasing the number of parareal iterations does not improve the accuracy of the solution beyond that of the coarse integrator. Finally, in the regions with large instabilities the solution is no longer useful. However many of the instabilities that lie inside the convergence regions are so small in magnitude that they do not appear prominently in the accuracy plots, since they will only affect accuracy after many steps of parareal.

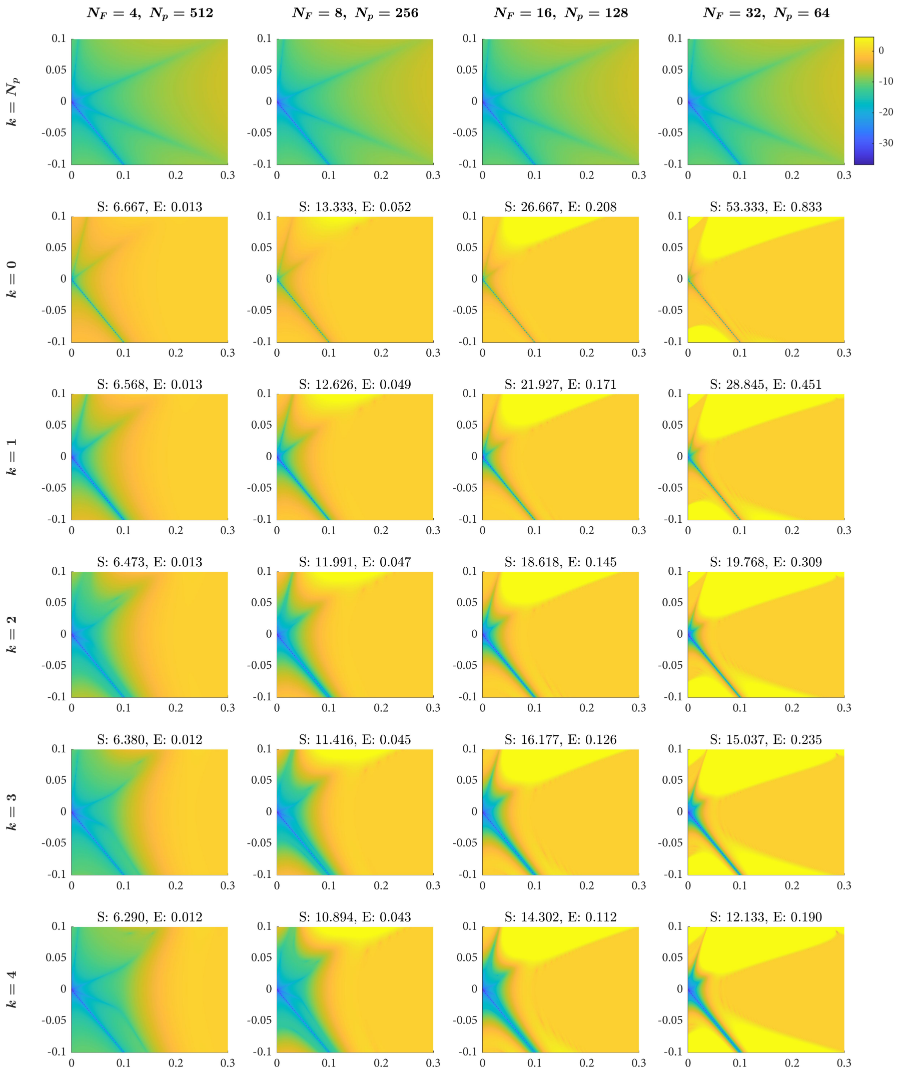

Fig. 4. Accuracy regions for parareal with a block size of $N_T = 2048$ and IMEX-RK3, IMEX-RK4 as the coarse and fine integrator. These plots complement the stability plots in Figure 3. The top row shows the accuracy of the fine integrator, the second row shows the coarse integrator, and all subsequent rows show the results of the number of increasing the parareal iterations. Color represents the log of the absolute value of the error.

5 Numerical experiments

The aim of our numerical experiments is to validate the results from linear stability analysis and demonstrate that we can obtain meaningful parallel speedup with IMEX-RK parareal on a dispersive equation. In particular, we show that:

1. taking too many parareal iterations leads to an unstable method; however larger block sizes N_T increase the range of stable choices for the iteration count k,
2. decreasing the number of processors for a fixed block size N_T eventually leads to an unstable method,
3. adaptive parareal method are effective so long as one limits the maximum number of iterations in order to avoid instabilities.

For our model nonlinear problem we select the one dimensional nonlinear Schrödinger (NLS) equation

$$\begin{aligned} &iu_t + u_{xx} + 2|u|^2 u = 0, \\ &u(x, t = 0) = 1 + \tfrac{1}{100}\exp(ix/4), \quad x \in [-4\pi, 4\pi]. \end{aligned} \tag{24}$$

We equip NLS with periodic boundary conditions, and use the method of lines with a fixed spatial grid. For the spatial component, we use a Fourier spectral discretization with 1024 points. In the time dimension we apply IMEX parareal methods that treat the linear derivative term implicitly and the nonlinear term explicitly. We solve the equation in Fourier space where the discrete linear derivative operators are diagonal matrices, and the implicit solves amount to multiplications with a diagonal matrix.

This solution of this problem has a subtle behavior when used as a test for a parallel in time method because the solution starts out very smooth but turns fully nonlinear around $t = 10$ due to temporary exponential growth in the mode $\exp(ix/4)$. We integrate (24) out to time $t = 15$ using $N_S = 2^p$ timesteps where $p = 7, \ldots, 18$. For parareal configurations with a large block size, we choose the first p so that the smallest timestep is at least as large as the block size. For brevity we only consider parareal integrators with IMEX-RK3 as the coarse integrator and IMEX-RK4 as the fine integrator. We also include a serial implementation of the fine integrator as a reference.

Finally, for all the plots shown in this section, the relative error is defined as $\|\mathbf{y}_{\text{ref}} - \mathbf{y}_{\text{method}}\|_\infty / \|\mathbf{y}_{\text{ref}}\|_\infty$ where $\mathbf{y}_{\text{ref}}$ is a vector containing the reference solution in physical space and $\mathbf{y}_{\text{method}}$ is a vector containing the output of a method in physical space.

5.1 Varying the block size N_T and the number of blocks N_b

In Figure 5 we present plots of relative error versus stepsize for multiple parareal configurations with different block sizes N_T. Each of the configurations has $N_F = 16$ and takes a fixed number of parareal iterations. The results demonstrate that increasing the block size leads to an improvement in stability that allows for a larger number of parareal iterations.

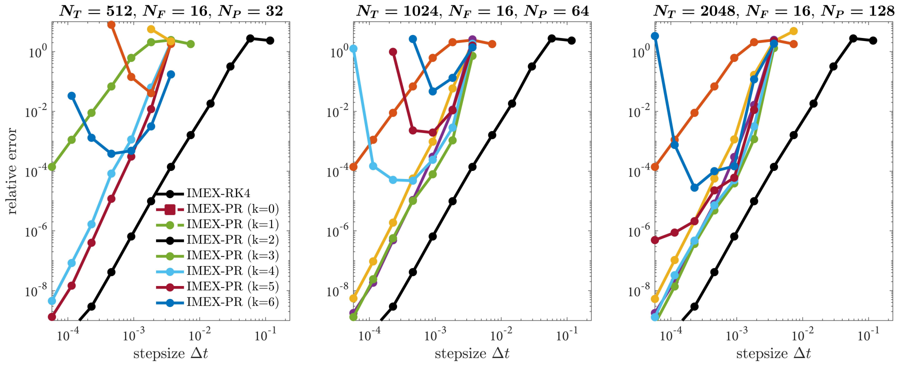

Fig. 5. Accuracy vs stepsize plots for the parareal method with IMEX-RK3, IMEX-RK4 as the coarse and fine integrator. The block size N_T for the left, middle, and right plots is respectively 512, 1024, and 2048. The black line shows the fine integrator run in serial, and the remaining colors represents a parareal method where each block takes a different number of iterations in each block.

The stability regions for the parareal configurations with $N_T = 512$ and $N_T = 2048$ are shown in the third columns of Figures 2 and 3. From linear stability we expect that the two parareal methods will respectively become unstable if $k > 3$ or $k > 4$. The experiments with $N_T = 512$ align perfectly with the linear stability regions. For the larger block size, the instabilities are milder and we would need to take many more parareal blocks for them to fully manifest. Nevertheless the methods fail to become more accurate for $k = 4$ and start to diverge for $k > 4$.

5.2 Varying N_p for a fixed N_T

Linear stability analysis shows that decreasing the number of processors N_p or equivalently increasing the the number of fine steps N_F will lead to an unstable parareal method if the block size N_T is kept constant. To validate this claim on a nonlinear problem, we consider four parareal methods with $N_T = 512$, $k = 3$, and $N_p = 16$, 32, 64, or 128. The linear stability regions for each of these methods are shown in the fourth row of Figure 2. Only the parareal method with $N_p = 128$ is stable along the entire z_2 axis. The method with $N_p = 64$ has a mild instability located inside its convergence region, and methods with $N_p = 32$ or $N_p = 16$ have large instabilities.

In Figure 6, we show an accuracy vs stepsize plot that compares each of the four

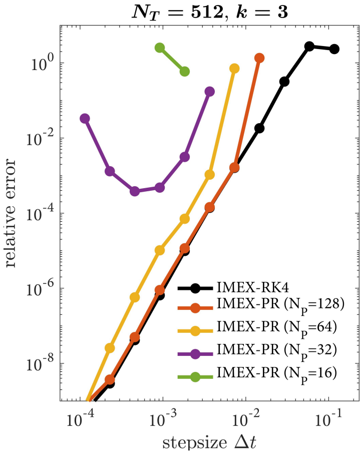

Fig. 6. Variable N_p results.

parareal configurations. The black line shows the serial fine integrator, and each color represents a parareal method with a different number of processors N_p. We can clearly see that decreasing N_p rapidly leads to instability. For $N_p = 64$ the instability is so small that it does not affect convergence in any meaningful way.

5.3 Efficiency and adaptive k

In our final numerical experiment we compare the theoretical efficiency of IMEX parareal to that of the serial fine IMEX integrator. To compute the theoretical runtime for parareal, we divide the actual run time of the fine integrator by the theoretical parareal speedup (13). This number represents the running time of parareal in the absence of any communication overhead.

In Figure 7 we show relative error versus computational time plots for both these experiments. The efficiency plots demonstrate that it is possible to achieve meaningful parallel speedup using IMEX parareal on the nonlinear Schrödinger equation. Amongst all the methods, the parareal configuration with $N_T = 2048$ and $k = 3$ was the most efficient.

In Figure 7 we also show a comparison between parareal with a fixed number of iterations and a parareal implementation that adaptively selects k in each block. In particular we compare the most efficient fixed parareal method to an identical parareal method with adaptive k. However, we note that it was necessary to restrict the maximum number of adaptive parareal iterations or the adaptive controller caused the method to become unstable at large stepsizes, especially when the residual tolerance is small. As seen from our results, there is very little difference between the two methods, except at the finest timesteps where the adaptive implementation is able to take significantly fewer iterations. The modest increase in speedup is due to the fact that the $N_p\alpha$ term in (13) remains constant for the different configurations.

6 Summary and conclusions

We have introduced a methodology for categorizing the convergence and stability properties of a parareal method with pre-specified parameters. Our analysis combines a simple bound on the norm of the parareal iteration matrix with traditional stability analysis that recasts the parareal algorithm as a one-step RK method with many stages. The resulting stability convergence overlay plots highlight the key characteristics of a parareal method including: regions of fast and slow convergence, stable regions where convergence does not occur, and regions where instabilities will eventually contaminate the method output.

By searching through a wide range of IMEX parareal methods, we were able to identify several stable configurations that can be used to solve dispersive equations. Moreover, each of the configurations possessed the same characteristics: low iteration counts k, large block sizes N_T, and a large number of processors

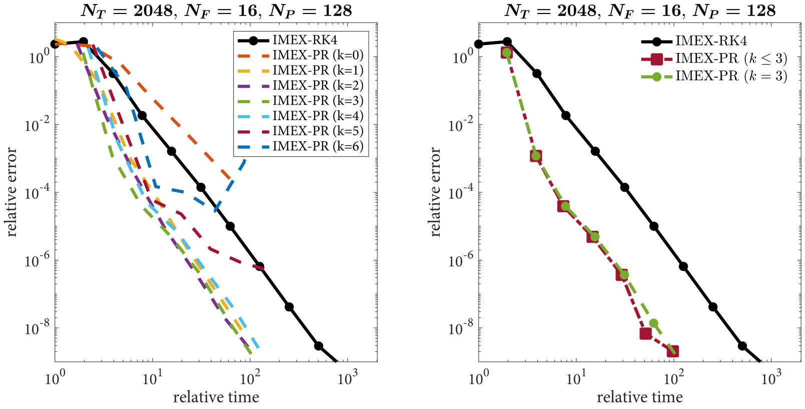

Fig. 7. Relative error versus computational time for the NLS equation solved using an IMEX parareal methods with $N_T = 2048$ and $N_p = 128$. The left plot compares seven parareal methods that take a different number of iterations per block. The right plot compares the most efficient fixed parareal method with $k = 3$ to a parareal method with adaptive controller where $k \leq 3$. In both plots, the black line show the fine integrator that is run in parallel. All times have been scaled relative to the fine integrator at the coarsest timestep.

N_p. We also observed that the most important factor that determines whether a parareal method is stable is the coarse integrator, and a bad choice can singlehandedly lead to an unstable method regardless of the other parameters.

More broadly, we see that convergence and stability regions are highly nontrivial and depend heavily on the parameters. It is clear that one cannot arbitrarily combine coarse and fine integrators and expect to obtain a good parareal method for solving dispersive equations. The same lesson also applies to all parareal parameters since serious instabilities can form by arbitrarily changing the number of iterations, the block size, or the number of processors.

Finally, we remark that the analysis presented in this work can be reused to study the properties of any Runge-Kutta based parareal method on the more general partitioned Dahlquist problem that represents both dispersive and diffusive equations. However, many of the conclusions and properties that we found are specific to IMEX methods and will not hold for different method families or for different problem types.

Acknowledgements

The work of Minion was supported by the U.S. Department of Energy, Office of Science, Office of Advanced Scientific Computing Research, Applied Mathematics program under contract number DE-AC02005CH11231. Part of the simulations were performed using resources of the National Energy Research Scientific

Computing Center (NERSC), a DOE Office of Science User Facility supported by the Office of Science of the U.S. Department of Energy under Contract No. DE-AC02-05CH11231.

References

1. U. M. Ascher, S. J. Ruuth, and R. J. Spiteri, *Implicit-Explicit Runge-Kutta methods for time-dependent partial differential equations*, Appl. Numer. Math., 25 (1997), pp. 151–167.
2. G. Bal, *On the Convergence and the Stability of the Parareal Algorithm to Solve Partial Differential Equations*, in Domain Decomposition Methods in Science and Engineering, R. Kornhuber and et al., eds., vol. 40 of Lecture Notes in Computational Science and Engineering, Berlin, 2005, Springer, pp. 426–432.
3. S. Boscarino and G. Russo, *On a class of uniformly accurate IMEX Runge–Kutta schemes and applications to hyperbolic systems with relaxation*, SIAM J. Sci. Comput., 31 (2009), pp. 1926–1945.
4. T. Buvoli, *Codebase for IMEX parareal stability plots*, (2020). `https://github.com/buvoli/imex-parareal`.
5. M. P. Calvo, J. De Frutos, and J. Novo, *Linearly implicit Runge-Kutta methods for advection-reaction-diffusion equations*, Appl. Numer. Math., 37 (2001), pp. 535–549.
6. A. Cardone, Z. Jackiewicz, H. Zhang, and A. Sandu, *Extrapolation-based implicit-explicit general linear methods*, (2013).
7. A. Dutt, L. Greengard, and V. Rokhlin, *Spectral deferred correction methods for ordinary differential equations*, BIT Numerical Mathematics, 40 (2000), pp. 241–266.
8. M. J. Gander, *Analysis of the Parareal Algorithm Applied to Hyperbolic Problems using Characteristics*, Bol. Soc. Esp. Mat. Apl., 42 (2008), pp. 21–35.
9. ———, *50 years of Time Parallel Time Integration*, in Multiple Shooting and Time Domain Decomposition, Springer, 2015.
10. E. Hairer, S. P. Nørsett, and G. Wanner, *Solving Ordinary Differential Equations I. Nonstiff Problems*, Math. Comput. Simul., 29 (1987), p. 447.
11. E. Hairer and G. Wanner, *Solving Ordinary Differential Equations II : Stiff and Differential-Algebraic Problems*, Springer Berlin Heidelberg, 1991.
12. C. A. Kennedy and M. H. Carpenter, *Additive Runge-Kutta schemes for convection-diffusion-reaction equations*, Appl. Numer. Math., 44 (2003), pp. 139–181.
13. J.-L. Lions, Y. Maday, and G. Turinici, *A "parareal" in time discretization of PDE's*, Comptes Rendus de l'Académie des Sciences - Series I - Mathematics, 332 (2001), pp. 661–668.
14. M. Minion, *Semi-implicit spectral deferred correction methods for ordinary differential equations*, Communications in Mathematical Sciences, 1 (2003), pp. 471–500.
15. J. Nievergelt, *Parallel Methods for Integrating Ordinary Differential Equations*, Commun. ACM, 7 (1964), pp. 731–733.
16. D. Ruprecht, *Wave Propagation Characteristics of Parareal*, Computing and Visualization in Science, 19 (2018), pp. 1–17.
17. G. A. Staff and E. M. Rønquist, *Stability of the parareal algorithm*, in Domain Decomposition Methods in Science and Engineering, R. Kornhuber and et al., eds., vol. 40 of Lecture Notes in Computational Science and Engineering, Berlin, 2005, Springer, pp. 449–456.

A Infinity norm of the parareal iteration matrix E

Let $\mathbf{A}(\gamma)$ be the lower bidiagonal matrix

$$\mathbf{A}(\gamma) = \begin{bmatrix} 1 & & & \\ \gamma & 1 & & \\ & \ddots & \ddots & \\ & & \gamma & 1 \end{bmatrix}.$$

Lemma 1. *The inverse of* $\mathbf{A}(\gamma)$ *is given by*

$$\mathbf{A}^{-1}_{i,j}(\gamma) = \begin{cases} (-\gamma)^{i-j} & j \leq i \\ 0 & \textit{otherwise} \end{cases}$$

Proof. For convenience we temporarily drop the γ *so that* $\mathbf{A} = \mathbf{A}(\gamma)$, *then*

$$\begin{aligned} \left(\mathbf{A}\mathbf{A}^{-1}\right)_{ij} = \sum_{k=1}^{N_p+1} \mathbf{A}_{ik}\mathbf{A}^{-1}_{kj} &= \begin{cases} 0 & j > i \\ \mathbf{A}_{ii}\mathbf{A}^{-1}_{ii} & i = j \\ \mathbf{A}_{ii}\mathbf{A}^{-1}_{ij} + A_{i,i-1}A^{-1}_{i-1,j} & j < i \end{cases} \\ &= \begin{cases} 0 & j > i \\ 1 & i = j \\ (-\gamma)^{i-j} + \gamma(-\gamma)^{i-1-j} & j < i \end{cases} \\ &= \begin{cases} 1 & i = j, \\ 0 & \textit{otherwise.} \end{cases} \end{aligned}$$

Lemma 2. *The product of* $\mathbf{A}(\omega)\mathbf{A}^{-1}(\gamma)$ *is*

$$\left(\mathbf{A}(\omega)\mathbf{A}^{-1}(\gamma)\right)_{ij} = \begin{cases} 0 & j > i \\ 1 & i = j \\ (-\gamma)^{i-j-1}(\omega - \gamma) & j < i \end{cases}$$

Proof.

$$\begin{aligned} \left(\mathbf{A}(\omega)\mathbf{A}^{-1}(\gamma)\right)_{ij} &= \sum_{k=1}^{N_p+1} \mathbf{A}_{ik}(\omega)\mathbf{A}^{-1}_{kj}(\gamma) \\ &= \begin{cases} 0 & j > i \\ \mathbf{A}_{ii}(\omega)\mathbf{A}^{-1}_{ii}(\gamma) & i = j \\ \mathbf{A}_{ii}(\omega)\mathbf{A}^{-1}_{ij} + \mathbf{A}_{i,i-1}(\omega)\mathbf{A}^{-1}_{i-1,j}(\gamma) & j < i \end{cases} \\ &= \begin{cases} 0 & j > i \\ 1 & i = j \\ (-\gamma)^{i-j} + \omega(-\gamma)^{i-1-j} & j < i \end{cases} \end{aligned}$$

Lemma 3. *The infinity norm of the matrix* $M(\omega,\gamma) = \mathbf{I} - \mathbf{A}(\omega)\mathbf{A}^{-1}(\gamma) \in \mathbb{R}^{N_p+1,N_p+1}$ *is*

$$\|\mathbf{M}(\omega,\gamma)\|_\infty = \frac{1-|\gamma|^{N_p}}{1-|\gamma|}|\gamma-\omega|.$$

Proof. Using Lemma 2, the j*th absolute column sum of* $M(\omega,\gamma)$ *is*

$$c_j = \sum_{k=j+1}^{N_p+1} |(-\gamma)^{k-j-1}(\omega-\gamma)| = \sum_{k=1}^{N_p-j} |(-\gamma)^k||(\omega-\gamma)|$$

It follows that $\max_j c_j = c_1$*, which can be rewritten as*

$$\frac{1-|\gamma|^{N_p}}{1-|\gamma|}|\gamma-\omega|.$$